How to cite: *Angew. Chem. Int. Ed.* **2022,** *61*, e202200755
International Edition: doi.org/10.1002/anie.202200755
German Edition: doi.org/10.1002/ange.202200755

Electrocatalysis

The Influence of Nanoconfinement on Electrocatalysis

Johanna Wordsworth, Tania M. Benedetti, Samuel V. Somerville, Wolfgang Schuhmann, Richard D. Tilley, and J. Justin Gooding**

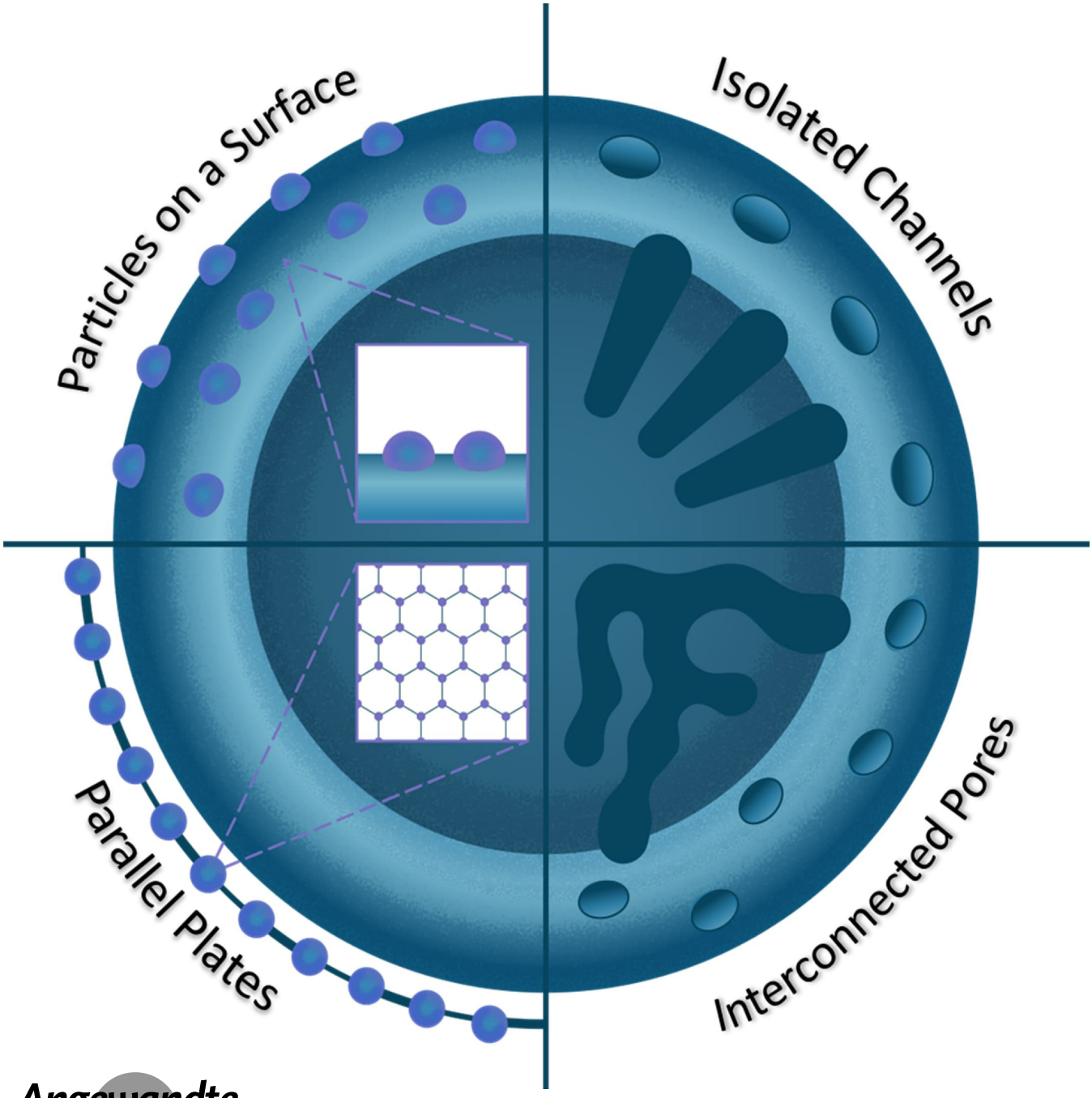

Abstract: The use of nanoparticles and nanostructured electrodes are abundant in electrocatalysis. These nanometric systems contain elements of nanoconfinement in different degrees, depending on the geometry, which can have a much greater effect on the activity and selectivity than often considered. In this Review, we firstly identify the systems containing different degrees of nanoconfinement and how they can affect the activity and selectivity of electrocatalytic reactions. Then we follow with a fundamental understanding of how electrochemistry and electrocatalysis are affected by nanoconfinement, which is beginning to be uncovered, thanks to the development of new, atomically precise manufacturing and fabrication techniques as well as advances in theoretical modeling. The aim of this Review is to help us look beyond using nanostructuring as just a way to increase surface area, but also as a way to break the scaling relations imposed on electrocatalysis by thermodynamics.

1. Introduction

Nanoconfinement is beginning to attract interest as a strategy for influencing electrocatalytic performance and, hence, it is crucial to understand the impact of nanoconfinement on electrocatalytic processes. In fact, an important review by Montoya et al.[1] proposed nanoconfinement as one of six strategies to break the scaling law limitation. By definition, nanoconfinement is confinement in a nanosized region, with the prefix nano- commonly described as being of dimensions less than 100 nm. From a functional perspective for electrocatalysis, nanoconfinement can be better described as confined regions where the solution environment is different to that observed at a macroscale surface. Such differences could present themselves as changes in reactant adsorption energies[2] or as changes in electrolyte composition[3] and reactant concentration[4] as a consequence of changes in the mass transport of reactants and products to and from the electrode surface.

Nanoconfinement is of such interest as it can provide benefits above the common paradigm of electrocatalysis in thinking that it is dominated by the Sabatier principle. The Sabatier principle focuses on the optimal catalyst having a balance between adsorption energies, so reactants bind, but not too strongly so as to allow bonds to dissociate and the products leave the surface.[5] Implicit in this principle is that the optimal binding energy pertains to the rate-determining step. The optimisation of a catalyst based on adsorption energies, however, has a theoretical limit. This limit in catalysis development arises when the same bonds are involved in the adsorption of reactants and desorption of products, and this is referred to as the linear scaling law limitation.[1,6]

To further enhance the activity of a catalyst beyond optimising binding energies, a common approach is to increase the number of exposed active sites by increasing the surface area by using nanostructures. This nanostructuring often results in confined spaces between the solid material.[7] A key question this Review aims to shed light on is how significant is the existence of these nonconfined spaces on electrocatalytic performance? As a consequence of the emphasis in electrocatalysis on the Sabatier principle, the enhancement we often see when using nanostructured electrocatalysts is sometimes attributed to electronic effects.[8] Although the effects of electronics should not be dismissed, other effects, including increased collisions due to short diffusion lengths, steric hinderance, reactant accumulation, and electrical double layer overlapping that can arise in nanoconfined spaces, should also not be overlooked.[7] Synthesising or fabricating experimental systems with well-defined nanoconfinement, however, can be challenging and our understanding of nanoconfinement in electrocatalysis is in its infancy.

Recently, it has become evident that nanoconfinement in highly porous electrocatalysts may also be contributing to improvements in the specific activity of electrocatalysts. In fact, there are studies that show nanoconfinement is the predominant factor in influencing the selectivity and kinetics of electrochemical reactions.[4a,d] In this Review, we first give an overview of nanostructures, grouped by their relative degree of nanoconfinement freedom, with examples highlighting how the electrocatalytic performance is affected by the presence of nanoconfined spaces. In subsequent sections, we discuss fundamental aspects of electrochemistry under nanoconfinement and how the different extents of confinement that these nanostructures bring affects electrocatalysis.

2. Overview of Nanoconfined Systems

Electrocatalytic systems with elements of nanoconfinement that contribute to electrocatalytic performance are becoming more widespread in the literature.[7,9] The extent of nano-

[*] J. Wordsworth, Dr. T. M. Benedetti, S. V. Somerville, Prof. J. J. Gooding
School of Chemistry, Australian Centre for NanoMedicine
University of New South Wales
Sydney 2052 (Australia)
E-mail: justin.gooding@unsw.edu.au
Prof. W. Schuhmann
Analytical Chemistry—Center for Electrochemical Sciences (CES)
Faculty of Chemistry and Biochemistry,
Ruhr University Bochum
Universitätstrasse 150, 44780 Bochum (Germany)
E-mail: wolfgang.schuhmann@rub.de
Prof. R. D. Tilley
Electron Microscope Unit, Mark Wainwright Analytical Centre
University of New South Wales
Sydney 2052 (Australia)

confinement is determined not only by the spacing between opposite sides of a channel or pore, but also by the degree of freedom by which a species can enter and leave the nanoconfined space. As such, we categorise nanoconfined systems based on their degree of freedom. The lower the degree of freedom, the greater the confinement of the electrocatalytic system. We will discuss four scenarios, as depicted in Figure 1a.

2.1. Nanoconfinement between Particles, Pillars, and Branches

Architectures that potentially exhibit some nanoconfinement, but possess the highest degree of freedom, include nanowires, closely spaced nanoparticles on an electrode, or nanoparticles with branches or spikes (Figure 1a). Mass transport between the confined regions and the bulk solution is largely unimpeded, with the effects of nanoconfinement only experienced when the solution species are located between closely spaced protrusions. The effects from nanoconfinement were demonstrated theoretically by Chang and co-workers,[2a] who showed that the faradaic efficiency for the CO_2 reduction reaction (CO_2RR) to CO

Johanna Wordsworth received her bachelor's degree in Nanoscience (Honours) at the University of New South Wales, Australia, in 2018. She is currently pursuing her PhD there under the supervision of Prof. J. Justin Gooding and Prof. Richard Tilley. Her research focuses on how nanoconfinement affects the activity and selectivity of electrocatalytic reactions.

Tania Benedetti received both her bachelor's degree in Chemistry in 2005 and PhD in Physical chemistry in 2011 from the University of Sao Paulo, Brazil. After a postdoctoral position at the University of Sao Paulo, she moved to Australia in 2014 to work as a postdoctoral fellow at the University of Wollongong and the University of New South Wales. She is currently a Lecturer at Griffith University, Australia. Her research interests are focused on understanding fundamental aspects of electrochemistry applied to batteries, electrocatalysis, and biosensing.

Samuel Somerville received his bachelor's degree in Nanoscience (Honours) at the University of New South Wales, Australia, in 2020. He is currently pursuing his PhD there under the supervision of Prof. J. Justin Gooding and Prof. Richard Tilley. His research focuses on controlling the nanoconfined solution environment for improved catalysis and sensing.

Wolfgang Schuhmann studied chemistry at the University of Karlsruhe and completed his PhD in 1986 at the Technical University of Munich. After finishing his habilitation at Technical University of Munich in 1993, he was appointed professor for Analytical Chemistry at the Ruhr University Bochum in 1996. His research interests cover a broad spectrum of different fields of electrochemistry, including biosensors, biofuel cells, batteries, photoelectrochemistry, electrocatalysts for energy conversion including high-entropy materials, scanning electrochemical microscopy, scanning electrochemical cell microscopy, in situ electrochemistry/spectroscopy techniques, and micro- and nanoelectrochemistry.

Richard Tilley received his master of chemistry from Oxford University, then completed his PhD in the same field at the University of Cambridge, after which he was a Postdoctoral Fellow at the Toshiba Basic R&D Center, Tokyo. He is the Director of the Electron Microscope Unit and in the School of Chemistry at the University of New South Wales (UNSW), Australia. Before working at UNSW, he was based at Victoria University of Wellington in New Zealand. His research focuses on the solution synthesis and electron microscopy characterisation of nanoparticles and quantum dots for applications ranging from catalysis to biomedical imaging.

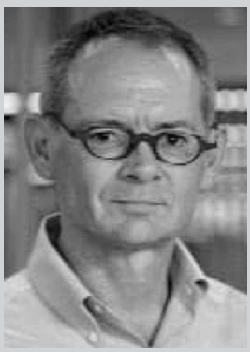

Justin Gooding graduated with a BSc (Hons) from Melbourne University, completed a DPhil at the University of Oxford, and received postdoctoral training at the Institute of Biotechnology in Cambridge University. He returned to Australia in 1997 as a Research Fellow at the University of New South Wales and became a full professor in 2006. He is currently a National Health and Medical Research Council Leadership Fellow and the Editor-in-Chief of ACS Sensors. He leads a research team of 45 people interested in surface modification and nanotechnology for biosensors, biomaterials, electrocatalysis, and 3D bioprinting.

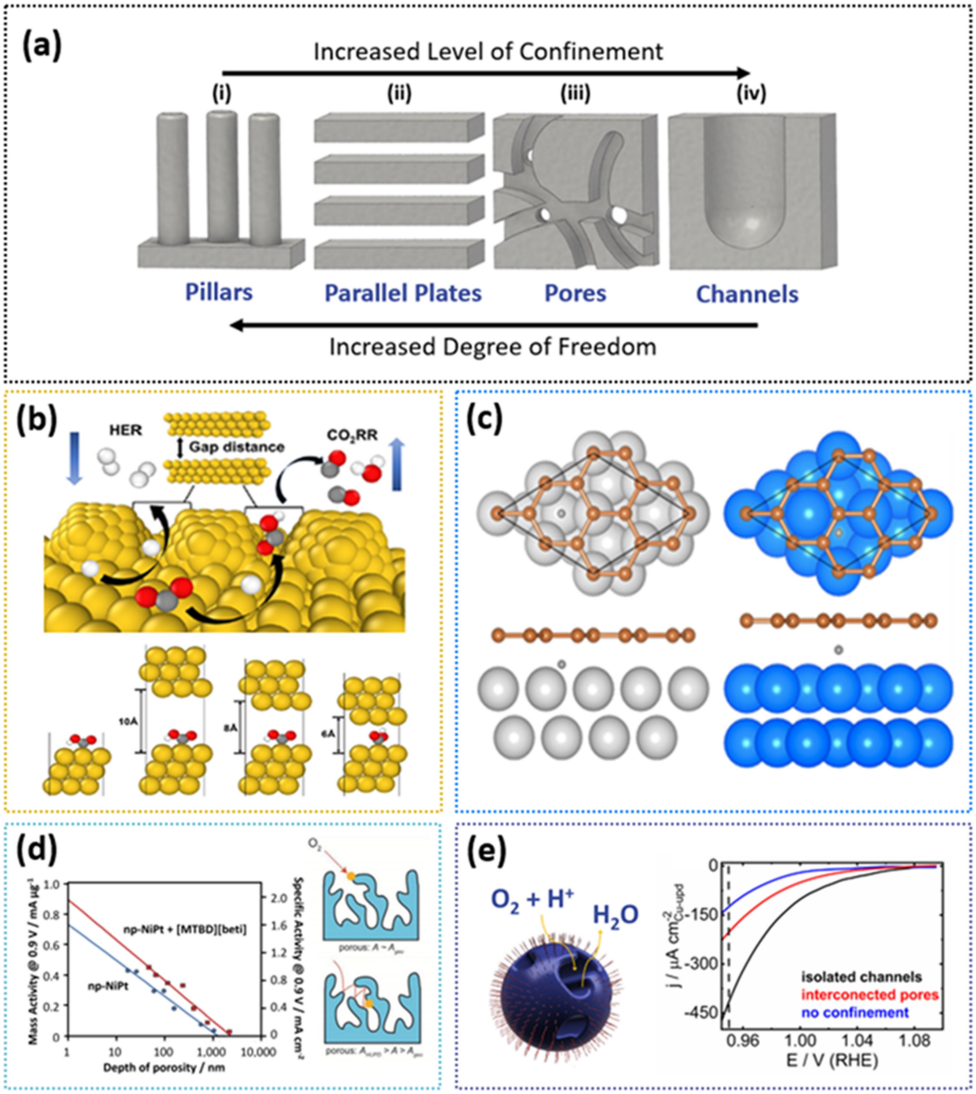

Figure 1. Types of nanoconfined systems. a) Schematic representation of nanoconfined systems: i) nanowires and pillars, ii) parallel plates, iii) interconnecting meso- and nanopores, and iv) an isolated channel system. b) Computational model of the confined microenvironment for the CO_2RR with two adjacent nanoparticles, where the configuration of *COOH is optimised within the confined structure, where the gap *d* is infinite, 10 Å, 8 Å, and 6 Å. c) Top and side views of the H adsorption configurations on graphene-covered metal surfaces for Ni and Cu (left) as well as Pd, Rh, Pt, Au, and Ag (right) substrates. d) Kinetic mass and specific activities at 0.9 V (RHE) for porous NiPt films with and without ionic liquid as a function of the dealloyed depth. Representation of the ORR on porous electrodes at both high (top) and low (bottom) overpotential. e) Schematic representation of nanozyme nanoparticles with passivated exterior surfaces and catalytic active sites inside substrate channels, together with a voltammogram displaying the specific activity for the ORR on spherical nanoparticles with isolated channels (nanozymes), interconnected pores, and no confinement, at low overpotentials. Adapted, with permission, from: b) Ref. [2a], Copyright 2020 American Chemical Society; c) Ref. [2c], Copyright 2016 American Chemical Society; d) Ref. [13], Copyright 2010 Nature; e) Ref. [15], Copyright 2018 American Chemical Society.

over the competing hydrogen evolution reaction (HER) was improved.

This was attributed to the stabilisation (increased adsorption energy) of the key reaction intermediate (*COOH) through its van der Waals interactions with the confining surface (Figure 1b) in nanoconfined spaces between Au and Ag nanoparticles. Nesselberger et al.[2b] has also observed by modelling an increased specific activity for the oxygen reduction reaction (ORR) occurring between proximal Pt nanoparticles as a result of a decrease in the adsorption energy of oxygen caused by double layer overlap in the nanoconfined region. They suggest that overlapping electrical double layers decrease the potential drop in the space between nanoclusters that have sufficiently small edge-to-edge distances. This decreases the adsorption strength, and hence coverage, of oxygenated species on the electrode surface, thereby resulting in a sharp increase in specific activity for the ORR as the edge-to-edge distance between particles decreases.

Ma and co-workers[3a] have shown selectivity for C_{2+} products in the CO_2 reduction reaction with Cu nanowire arrays of various lengths and densities. This was attributed

to the higher local pH value in the nanoconfined spaces compared to the bulk pH caused by hindered diffusion of HCO^{3-} into, and produced OH^- out of, the Cu dense nanowire array. Higher local pH values can both hinder the HER and facilitate the reduction of the intermediate CO to C_2H_4, C_2H_6, ethanol, and propanol.[10] Hence, the nanoconfinement within high-density nanowire arrays can locally counteract the buffering ability of the electrolyte solution, thus increasing the local pH value and promoting the formation of such products. In a contrasting example, Myekhlai et al.[11] highlighted using Pd-core Ru-branched nanoparticles for the oxygen evolution reaction (OER), whereby the produced oxygen bubbles become entrapped in the nanoconfined spaces and effectively limit the electrolyte/catalyst interface. This became more prominent when the branch number per nanoparticle was increased such that the spacing between branches decreased.

2.2. Nanoconfinement between Two Parallel Planes

This geometry restricts the movement of species to the space between the planes, thereby decreasing the degree of freedom compared to nanowires (Figure 1a). An example of how the level of nanoconfinement arising from this geometry affects electrocatalytic reactions was given by Zhou et al.[2c] when looking with DFT calculations at combinations of graphene-covered metallic surfaces for the HER (Figure 1c). Different HER rates compared to their bare metal counterparts were observed, which was attributed to the weakened adsorption of hydrogen when it is confined between the graphene and metal surfaces. This was observed for all the metals investigated and was attributed to both the energy penalty caused by lifting the graphene overlayer to provide enough space for the adsorbed H atoms and graphene pushing the H atoms to be closer to the metal.

Yao et al.[2d] also observed weakened CO adsorption by the presence of a graphene overlayer on a Pt surface using simulations and DFT calculations. The overlayer facilitates CO oxidation with a lower apparent activation energy compared to a bare Pt surface. The sub-nanometer distance between the graphene overlayer and the metal substrate allows charge transfer between graphene and the CO and O adsorbates to weaken the C–O bond, thereby promoting the formation of the O–CO bond during CO oxidation. Experimental results by Zhang et al.[2e] supports the studies above. With a Pt surface under a 2D hexagonal boron nitride (h-BN) overlayer, CO adsorption on Pt was significantly weakened because of confinement in between the layers alleviating the CO poisoning effects and, hence, facilitating CO oxidation at the interface. Within their study, the authors compared the decrease in the adsorption energy seen when using a h-BN overlayer compared to a graphene overlayer, and they suggest that it is the electronic interaction between the overlayer and the metal surface that determines the influence of the confinement effect. A more significant decrease is seen for the polar h-BN sheet, which may interact more strongly with the metal substrate than the nonpolar graphene.

2.3. Nanoconfinement in Mesoporous Nanoparticles and Films

Mesoporous films and nanoparticles are the most common structures investigated experimentally. These materials have interconnected pores and, thus, an even lower degree of freedom compared to the previous two geometries (Figure 1a). This is because a solution species entering the mesoporous environment can only move along the pore spaces, thereby resulting in noticeable changes in the solution environment compared to the bulk solution. A 3D system comprised of interconnected mesopores, however, can still be thought of as a single mass-transport system (Figure 2b) as distinct from the parallel plates or completely isolated nanopores (see below), where each nanoconfined space is a separate mass-transport system (Figure 2c,d). There are important consequences of this difference, including more facile diffusion as a result of higher accessibility for species to enter and leave unimpeded.[12]

This type of confined system with interconnected, open pores can provide a different solution environment to the bulk solution, which can impact both the activity and selectivity. Using porous Ni–Pt surfaces, Benn et al.[4c] demonstrated selectivity for the ORR even in the potential ranges normally dominated by the hydrogen evolution reaction (HER), which was ascribed to the depletion of H^+ ions inside the nanopores hindering the HER, whereas oxygen reduction proceeds through a water dissociation mechanism not requiring H^+ ions. Porous geometries can also act as a sieve to exclude larger species, as shown by Ding et al.[3b] for nickel nanostructures within a silica nanochannel membrane for the oxidation of glucose. The 2–3 nm diameter silica channels enabled molecular selectivity by blocking large biofouling molecules and allowing small glucose molecules to permeate through the channels, thereby resulting in increased sensitivity and a low limit of detection.

Snyder et al.[13] observed that both ORR mass transport and specific activity increase as the depth of the Pt–Ni surface porosity decreases (Figure 1d (left)). They hypothesised that the active surface area of porous electrodes may not always equal the surface area determined by H_{UPD}, and that the active area may be a function of potential. At high overpotentials (Figure 1d (top)), the active area is effectively equal to the electrode geometric area, as nearly all reactant–

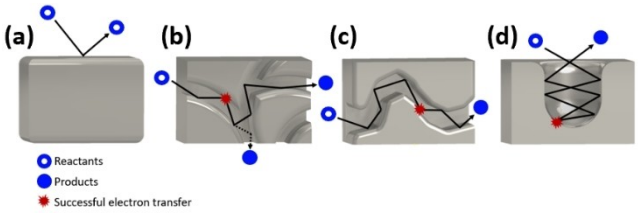

Figure 2. Increased collisions as a result of nanoconfined space. Schematic depiction of a) a planar electrode, where reactants often only interact with the surface once before diffusing back into the bulk electrolyte; a mesoporous sheet of b) interconnected pores, and c) non-interconnected pores, both acting as "partition membranes"; and d) an isolated channel only open at one end.

substrate interactions result in electron transfer. However, in porous materials at low overpotentials (Figure 1d (bottom)), the 2 nm diameter pores increased the frequency of collisions and, hence, enhanced the probability of electron transfer. Less reactant depletion also means that that oxygen can reach further into the porous geometry, thereby resulting in a higher electroactive surface area.

2.4. Nanoconfinement in Isolated Channels

This is the most confined geometry, with the fewest degrees of freedom (Figure 1a). Similar to the planar geometry, where each parallel plate is isolated from the others, once a species diffuses into an isolated channel, it is not only restricted from entering another channel, but the species in one channel is not influenced by species in adjacent channels. Similar to the mesoporous systems mentioned above, the collision frequency in isolated channels is significantly augmented compared with a planar surface (Figure 2a). Isolated channels experience less facile diffusion compared to pores, as there is only one opening for reactants and products to enter and exit (Figure 2d), so each isolated channel is a separate discrete diffusional system with each channel forming a steady-state flux.

Improved selectivity for the CO_2RR with isolated channels was shown by Yang et al.,[14] who developed an array of isolated Cu channels with tunable depths and widths. Different channel dimensions resulted in different retention times of species in the channels, with longer and narrower pores showing increased faradaic efficiency for C_2 over C_1 products. Similarly, Zhuang et al.[4d] showed the formation of C_3 products from the reduction of CO inside hollow Cu nanoparticles, which can be regarded as being a single channel in a nanoparticle, by concentrating C_2 species through steric confinement and promoting the coupling of C_2 and C_1 intermediates.

Recently, our group synthesised Pt–Ni particles with isolated channels resembling the substrate channels in enzymes.[4a,15] The outside surface remained passivated with a hydrophobic surfactant, thereby allowing the ORR to occur only inside the isolated channels (Figure 1e). The specific activity inside the channels was three times higher than the activity on the nanoparticle external surface and two times higher than nanoparticles with interconnected mesopores of similar confined space diameters. This was attributed to a higher concentration of reactant species at low overpotentials. By comparing no confinement, interconnected pores, and isolated channels (blue, red, and black in Figure 1e, respectively), this study is the first demonstration of how different levels of confinement affect the activity.

What emerges from this overview is that many nanomaterials and nanostructured surfaces are being synthesised as electrocatalysts, with phenomenological experimental studies attributing observations to nanoconfinement and theoretical papers describing nanoconfinement effects. The study of nanoconfinement in electrocatalysis has not yet reached the maturity of designing experiments based on theoretical studies. This is partly a consequence of the challenges in fabricating nanoconfined systems that are sufficiently well-defined to test the theoretical predictions and the complexity of the modeling studies when including mass transport, changes in the solution environment, adsorption behavior, electrostatics, and reaction kinetics. Recent developments in materials design have enabled many nanoconfined systems to be synthesised. Covalent and molecular organic frameworks with highly ordered, sub-nanometer confinement and versatile properties,[16] liquid-crystal templates with a high degree of control to produce isolated channels of various heights and widths,[17] as well as carbon nanotubes[18] and other carbon allotropes have potential for very controlled studies into nanoconfinement. The variability in the nanoscale systems that can be fabricated at this stage does create some limitations on the types of questions that can currently be addressed in electrocatalysis, unlike in nanoconfined sensing systems that use biologically generated nanoconfined systems, such as protein nanopores, where subtle effects related to chemical bonding and chemical interactions can be studied.[19] Despite the limitations in questions that can be asked by our current capabilities to fabricate well-defined nanoconfined systems, some important knowledge regarding nanoconfinement in electrochemistry is emerging and will be discussed in the next sections.

3. Under what Electrochemical Conditions Are the Effects of Nanoconfinement Most Prominent?

Any influence of nanoconfinement on an electrochemical reaction will be most prominent when the reaction is limited by electron-transfer kinetics rather than mass transport. This is because in the mass-transport regime, reactants will be depleted in the nanoconfined spaces, thereby resulting in reactions only occurring on the exterior of a nanoporous material.[4a] Hence, depending on the electron-transfer kinetics relative to the rate of mass transport, not all the nanoconfined regions will be involved in the reaction. That is, under mass-transport control, the current from a porous electrode can converge to that observed at a planar electrode, as the internal pore space remains un-utilised in the reaction (Figure 3a (top)).[12b,20] Implicit in the assertion that nanoconfinement effects will be greatest in the kinetic regime is that the impact of nanoconfinement will be greater for reactions with sluggish reaction kinetics such that there is minimal reactant depletion inside the nanoconfined environment. In such cases, nanoporous electrodes will present larger specific activity than electrodes with less nanoconfinement, because of the higher number of collisions between the reactant and the electrocatalyst (Figure 2b–d). The Chung research group (Park et al.,[12b] Han et al.[20a]) showed this experimentally by comparing relatively fast (oxygen reduction) and slow (glucose oxidation) reactions on Pt. They found that, for the slower glucose oxidation reaction, increasing roughness resulted in increased current at high overpotentials as a result of an

increase in the electroactive surface area because the slow reaction very rarely attains the full mass-transport limitation (Figure 3a (bottom)). In contrast, the faster ORR experiences fast reactant depletion at high overpotentials, which results in a current plateau as the roughness factor increases (Figure 3a (top)).[12b] Hence, electrochemically facile reactions were shown to reach current saturation as the degree of porosity increased, whilst no such saturation in the enhancement induced by nanoconfinement is reached for slower reactions. The contribution of the increased surface area from nanopores can be eliminated by normalising the current with the electrochemically active surface area. At a low overpotential for the ORR, the specific activity is larger for the porous Pt electrode in comparison to the flat Pt electrode; however, the planar electrode becomes more active at high overpotentials because of O_2 depletion inside the nanoporous structure, which limits the reaction to its surface (Figure 3b).[20a] In addition to being in the kinetically limited regime, the strength of the adsorption of species also influences nanoconfinement. Reactions with weakly binding reactants experience the effects of nanoconfinement more significantly than strongly adsorbing ones because they can exploit the greater number of collisions between the reactant and the catalyst that the confined spaces facilitate.

Bae et al.[20b] demonstrated this with the electrooxidation of 1-butanol and 2-butanol on nanoporous Pt. As the probability of a collision resulting in electron transfer is higher for the strongly absorbing 1-butanol, the effect of nanoconfinement arising from the enhanced collision frequency in the nanoporous electrocatalysts, versus non-confined electrode materials, contributes less to the activity of the catalyst than for 2-butanol. At higher overpotentials, this results in lower specific activity for the porous electrode, relative to the planar electrode, as the reactant is mostly adsorbed and, hence, consumed, near the outside surface of the porous catalytic material (Figure 3c). In contrast, with the weakly binding 2-butanol, higher specific activity is obtained with the porous Pt than the planar electrode, as the increase in collision frequency within the nanoconfinement compensates for the lower probability of a collision resulting in adsorption and, hence, reaction. The result is an enhancement in the reaction kinetics (Figure 3d).

We recently showed that the effect of nanoconfinement is more dominant under kinetic control.[4a] The effect of the channel diameter on the ORR kinetics has shown that smaller channels are more active at lower overpotentials because of more confined spaces and higher reactant concentrations. However, larger channels, which are less confined, eventually become more active as the overpotential increases as they have a higher number of active sites at the entrance of the channel, which is where the ORR mostly happens when the reaction becomes diffusion-controlled. Note that in this study, all nanoparticles with nanoconfinement (Figure 3e) are always more active than those without (Figure 3f) within the potential range studied, which shows that nanoconfinement has an effect even under mixed kinetic mass transport control.

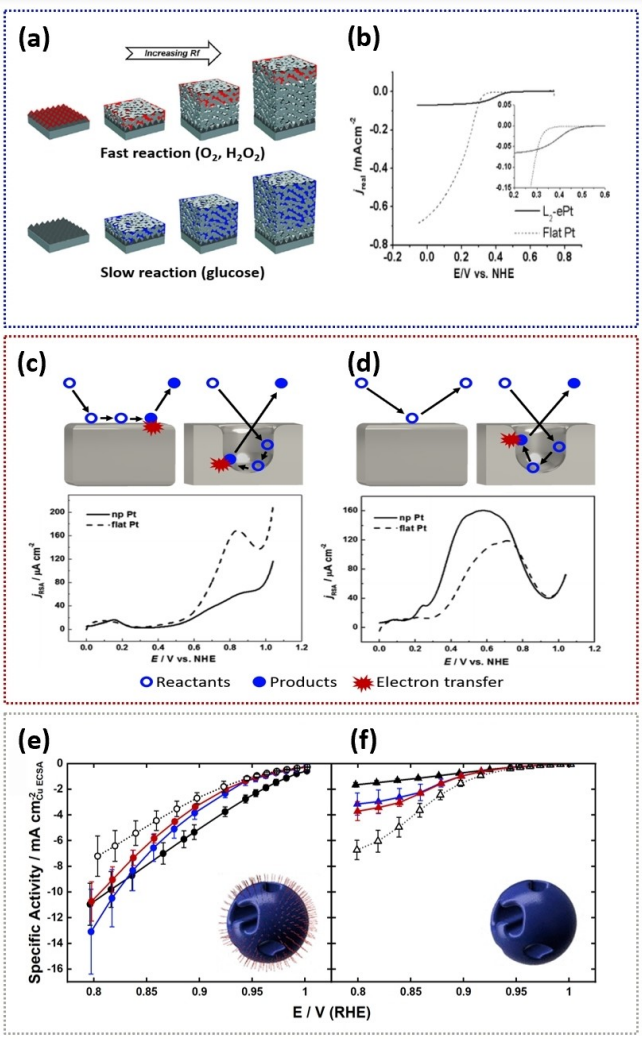

Figure 3. Conditions where nanoconfinement are most prominent. a) Schematic illustration of the volume of the porous electrode surface that participates in the reaction when the reaction is fast (mass transport limited, top) and slow (kinetically limited, bottom). b) Linear sweep voltammograms of a flat and porous Pt electrode in oxygen-saturated 0.1 M phosphate buffer containing chloride. Currents are normalised to the electrochemical surface area. The effect of the degree of adsorption on collision frequency as a result of nanoconfinement for c) adsorption reactions (e.g. oxidation of 1-butanol) and d) non-adsorption reactions (e.g. oxidation of 2-butanol). Kinetic current densities calculated from Koutecký–Levich plots at 0.8–1.0 V (RHE) for nanozymes with e) small (black), medium (blue), large (red) channels, and mesoporous particles (white); f) small channel particles without surfactant (black), medium channel particles without surfactant (blue), large channel particles without surfactant (red), and mesoporous particles without surfactant (white). Error bars represent the standard deviation from triplicate experiments. Adapted, with permission, from: a) Ref. [12b], Copyright 2010 Elsevier; b) Ref. [20a], Copyright 2010 American Chemical Society; c), d) Ref. [20b], Copyright 2013 Royal Society of Chemistry; e), f) Ref. [4a], Copyright 2020 Royal Society of Chemistry.

4. How Is Mass Transport Affected by Nanoconfinement?

Although the effects of nanoconfinement are more prominent when the reaction is under kinetic control, the effect on mass transport cannot be disregarded. The rate of mass transport, in particular diffusion and migration, has a strong dependency on the local solution environment. This is especially the case for sluggish reactions that will still be under a mixture of kinetic/mass transport control at relatively high overpotentials. Particularly important in altering the local concentration in nanoconfined volumes is the impact on the electrical double layer (EDL). If the radius of the nanoconfined space is less than twice the thickness of the EDL, then the double layers from both sides of the walls of the nanoconfined space overlap. This can be achieved by either decreasing the nanoconfined size or using an electrolyte with a lower ionic strength. This is shown in Figure 4a, where the concentration of counterions and co-ions in a 2 nm wide channel never become equal to the bulk concentration in 0.5 mol L^{-1} electrolyte, which results in an excess of counterions within the confined space.[21] In contrast, at high ionic strength, the counterion and co-ion concentration becomes equal in the centre of the channel, as the EDLs do not overlap (Figure 4b). This charge imbalance inside the channel can affect mass transport into the channel and will depend on whether the ions making the EDL participate or not in the electrochemical reaction. Diffusion is usually the dominant mode of mass transport in electrochemical reactions. However, when there is EDL overlap in confined spaces, and the species that make up the EDL are consumed in the reaction, an imbalance of charge is created that can cause counterions to be drawn into the nanoconfined space by migration. The mass transport of a charged reactant can either be enhanced or retarded by migration, depending on the charge of the reactant. In the case of the ORR, as the reduction potentials increase, H^+ ions are drawn from the bulk electrolyte into the channels by migration, thereby enhancing the reaction rate because of the higher flux of reactants and, hence, increased concentration near the electroactive surface (Figure 5a).[22]

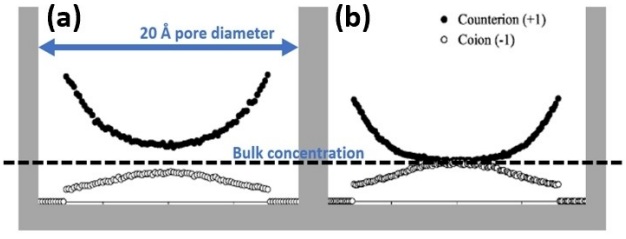

Figure 4. Concentration profiles in nanoconfined space. Counterion and co-ion concentration profiles in a 20 Å diameter nanopore for a single 1:1 electrolyte with a surface charge density of −0.05 C m^{-2} and an ionic strength of a) 0.5 mol L^{-1} and b) 1.0 mol L^{-1}. Adapted, with permission, from Ref. [21], Copyright 2008 AIP Publishing.

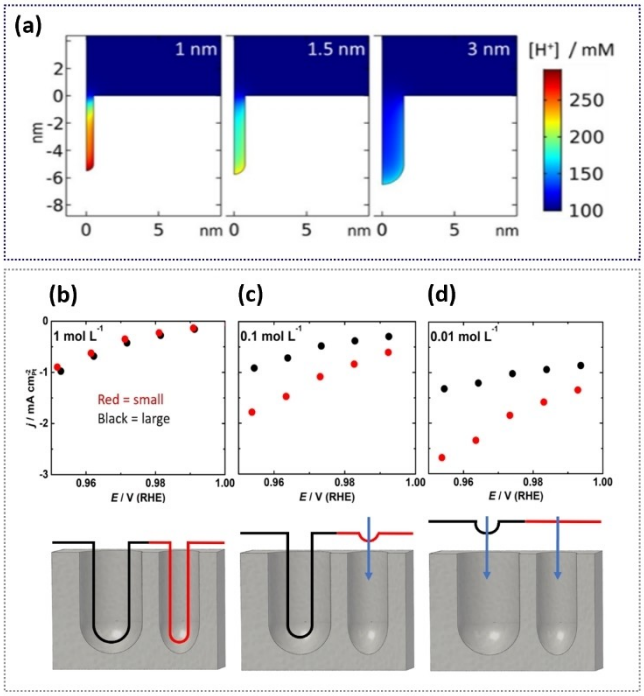

Figure 5. Electrical double layer overlapping in nanoconfined space. a) Simulated H^+ concentration distribution in 1 nm, 1.5 nm, and 3 nm diameter channels during the diffusion-limited reduction of oxygen, showing higher H^+ concentrations in narrower channels. The depletion of H^+ ions is insignificant regardless of the selected applied potential. Kinetic current densities for the ORR at 0.95–1.0 V (RHE) for nanozymes with small (< 2 nm; red) and large (> 2 nm; black) channels at different $HClO_4$ concentrations: b) 1.0 mol L^{-1}, c) 0.1 mol L^{-1}, and d) 0.01 mol L^{-1}. Each voltammogram is accompanied with a scheme, where the line represents the equipotential profile separating the EDL from the bulk solution, and the arrows represent migration into the channels when EDL overlapping occurs. Adapted, with permission, from Ref. [4a], Copyright 2020 Royal Society of Chemistry.

Migration will then be the most significant mode of mass transport for charged species as they cannot diffuse against the concentration gradient formed inside the nanoconfined space, whereas uncharged species do not have the benefit of migration as they can only be transported by diffusion. If the nanoconfined space is sufficiently wide, or the concentration of electrolyte is sufficiently high, there is no overlap of the EDLs, and the main mode of mass transport into the nanoconfined volumes will be diffusion. The species being consumed at the EDL can then be readily replaced by the ones in the bulk-like electrolyte located in the centre of the channel (scheme in Figure 5b), just as it does on a planar electrode.

Changing the size of the nanoconfined space can also affect the reaction kinetics as a result of strain caused by changes in curvature and coordination number[23] affecting the binding energy of species. Although the contribution of strain to the catalytic activity may still be important, experimental evidence shows that overlapping of EDLs can play a major role in nanoconfined isolated channels. This was shown by us with the same system described in Figure 1e. When H^+ ions in overlapped EDLs are consumed

during the ORR, higher specific activity at low overpotentials is seen due to increased migration of H^+ ions into the channel (Figure 5c, d). Changes in the degree of overlap of the diffuse double layers of the EDL by either changing the channel size or electrolyte concentration can be directly correlated with the specific activity. Interestingly, the activities were very similar in samples with different channel diameters (and, hence, differences in the degree of curvature and strain) when there was no EDL overlapping (Figure 5b), which suggests that the mass-transport effect is dominant.[4a]

In the example above, the effects of EDL overlapping on migration-facilitated mass transport was demonstrated with an isolated channel system. Although EDL overlapping can also occur in interconnected pores, the impact on specific activity is not as significant because the greater degree of freedom in the interconnected pores results in reactants not being accumulated to the same extent as in isolated channels.[24] This suggests that the effects of migration are more noticeable with isolated channels, where diffusion is restricted. We were able to demonstrate a greater effect of migration with isolated channels versus connected pores by comparing nanoparticles of identical size with both isolated channels and interconnected pores of similar sizes. Compared to a system with no confinement, the specific activity was 3.3 times greater in the nanoconfined system comprised of isolated channels, whereas a specific activity increase of only 1.7 times was seen for the interconnected pores (Figure 1e).[15]

Similar effects were even observed by Chen et al.[25] in systems that do not exhibit EDL overlapping through the use of a thin-layer electrochemical cell that was a few hundred nanometers wide. At supporting electrolyte concentrations low enough for the EDL to extend a significant distance into the solution, increased activity for the hexaaminеruthenium(III) chloride redox couple ($Ru(NH_3)_6^{3}/Ru(NH_3)_6^{2+}$) was observed. This was attributed to ion enrichment in the EDLs at the surface of the cathode caused by enhanced ion migration of the redox species. The use of recessed microelectrodes in this study allowed the beneficial effects of confinement to be seen even at mass-transport-limiting potentials.

In addition to inducing mass transport by migration, when the confined space and EDL dimensions are comparable, the physical properties of ions and the water structure become significant and can affect ion transport inside the confined environment. The mobility of H^+ ions is heavily influenced by the water structure, as the mechanism by which protons move involves a transfer of a single positive charge from one hydrogen-bonded water molecule to the next (Grotthuss mechanism). Highly ordered systems of water molecules, such as those found in Ångström-scale nanochannels, enhance the H^+ mobility along the axis of the nanochannels via a single layer of "frozen" water molecules traversing the nanopore and forming a highly orientated hydrogen-bonded chain.[18a,26] When comparing carbon nanotubes of 0.8 nm and 1.5 nm diameter, Tunuguntla et al.[18b] saw increased H^+ transport rates for the heavily confined 0.8 nm tube which, because of its size, formed a wire of single water molecules in a chain. This was not the case for the 1.5 nm channels, where the behaviour was more similar to that of bulk electrolyte. In contrast to the situation with nanoslits and nanochannels, Sofronov and Bakker[27] discovered that the mobility of H^+ ions in nanodroplets, where the movement of H^+ ions is confined in all three dimensions, is up to 10 times slower than in bulk water. This was ascribed to the fact that if a water molecule forms fewer than two hydrogen bonds then it cannot efficiently accept the H^+ ion because of decreased basicity, which increases the average residence time at each water molecule.

Ion transport can also be affected by nanoconfinement. Ions entering nanoconfined spaces of a few nanometers often need to partially shed their hydration layers. Ionic selectivity can arise from variations in hydrated radius and hydration strength (energy expenditure for dehydration) between different ions.[28] Whereas high ionic mobility in nanoconfined spaces at low ionic strength has been reported,[29] Ma et al.[30] found that at high electrolyte concentrations (>1 M), ion mobility is lower compared to the bulk because of an enhancement in the number of pairings and collisions between partially dehydrated ions of opposite charge inside the nanopore. Despite the presence of numerous experimental and theoretical contributions focusing on ionic and molecular mobility in confined systems, the literature is less developed for how this influences electrochemical reactions.

5. How Can Nanoconfinement Break Scaling Relationships?

As discussed in the introduction, the reaction overpotential can be minimised by optimising the binding energy of a key intermediate to ensure the binding is strong enough for successful electron transfer, but weak enough for the product to be immediately released from the catalytically active site. Binding energies can be tuned by surface faceting, elemental alloying, surface defects, and coordination numbers.[23,31] As mentioned previously, nanoconfinement itself can also be used to selectively weaken adsorption energies between the reactant and catalytic surface.[2a–e]

However, manipulating the binding energy of one intermediate will simultaneously affect the binding energy of other intermediates, possibly creating a new limiting step involving the other intermediate.[32] Thus, the manipulation of binding energies will not result in activities higher than that dictated by the scaling relations.

Nanoconfinement can break scaling relationships in two distinct ways. One way is by preferentially stabilising one adsorbed reaction intermediate while not affecting the adsorption of the other intermediates. Doyle et al.[2f] demonstrated this theoretically with adjacent RuO_2 and IrO_2 parallel plates for the OER [reaction mechanism shown in Eqs. (1)–(4)] and found that the effect of nanoconfinement depends on the rate-limiting step.

$$H_2O + M \rightarrow M{-}OH + H^+ + e^- \quad (1)$$

$$M{-}OH \rightarrow M{-}O + H^+ + e^- \quad (2)$$

$$M{-}O + H_2O \rightarrow M{-}OOH + H^+ + e^- \quad (3)$$

$$M{-}OOH \rightarrow M + O_2 + H^+ + e^- \quad (4)$$

The HOO* intermediate was stabilised by hydrogen-bond formation with the opposite channel wall, whereas no changes in the adsorption energy was seen for the smaller HO* intermediate. Reactions that fall on the right side of the volcano plot (Figure 6a (right)), namely, at IrO_2 surfaces, are rate-limited by the deprotonation of HO* to O* [Eq. (2), red line in Figure 6a (bottom)] when the spacing between plates is greater than 1 nm ($d > 1$ nm), which is not affected by confinement. However, when $d < 1$ nm, the rate-limiting step becomes the removal of HOO* from the IrO_2 surface [Eq. (4), blue line in Figure 6a (bottom)]. The stabilisation that arises from confinement hinders the removal of HOO* from the surface. Hence, for IrO_2, the overpotential for the OER increases as the channel size decreases. Conversely, on the left side of the volcano plot, namely, at RuO_2, reactions are potential-limited by the addition of a second water molecule to O* to form HOO* [Eq. (3), green line in Figure 6a (top)], so the increased stability of HOO* because of confinement results in an increased activity. The overpotential for RuO_2 decreases to about 200 mV at $d = 0.7$ nm and forms a new volcano plot, whose summit reaches closer to the currently unattainable 0 V overpotential. This approach can be used for other reactions involving multiple intermediates that have different spatial extension of their orbitals. Nearly identical results were obtained more recently by Sours et al.[33] using density functional theory calculations of bimetallic porphyrin-based MOFs, who demonstrated hydrogen-bonding stabilisation of the HOO* intermediate. The optimal separation between the two confining layers was found to be about 0.7 nm, and a decrease in the overpotential was seen for reactions whose rate is limited by the formation of HOO*.

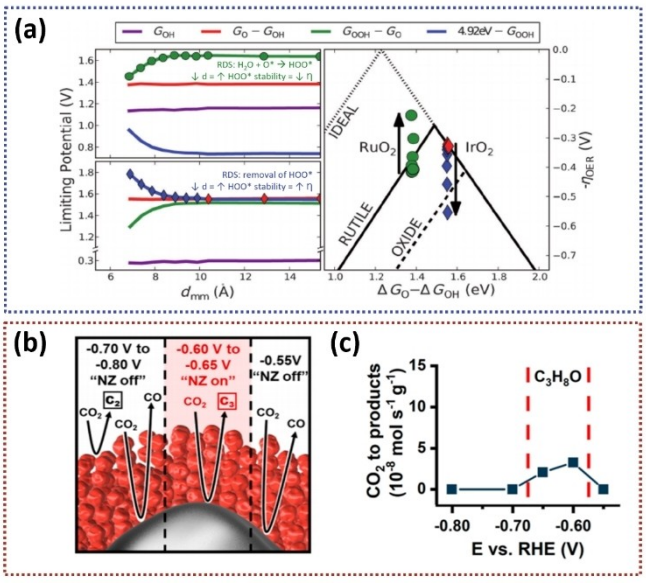

Figure 6. Breaking scaling relationships with nanoconfinement. a) The potential needed to drive each oxygen-evolution reaction step on RuO_2 (top) and IrO_2 (bottom) as a function of channel width. Discrete symbols represent the highest limiting potential in the plots on the left, which have been translated to overpotentials in the volcano plot on the right. Arrows indicate trends in activity as d_{mm} decreases. b) Schematic representation of processes occurring at the specific potential windows with active (red) or inactive (black) nanozyme cascade mechanisms, and c) product formation rates of C_3H_8O in moles per second and gram of nanozyme particles. The vertical lines separate three distinct potential windows. Adapted, with permission, from: a) Ref. [2f], Copyright 2015 European Chemical Societies Publishing, and b), c) Ref. [4b], Copyright 2019 American Chemical Society.

Another way nanoconfinement can break scaling relationships is by increasing the residence time of species near active sites in nanoconfined spaces, which leads to enhanced kinetics as well as the selective formation of more complex products in multiproduct reactions. For multistep, multiproduct reactions such as the CO_2RR, scaling relationships can be broken by using interfacial sites that each catalyse one step of the cascade reaction. Huang et al.[34] used nanodimer particles containing Ag and Cu to lower the overpotentials required for the CO_2RR, thereby increasing the selectivity for C_2 products. To obtain even higher order products, such as propanol, higher concentrations and long retention times of the C_2 and CO intermediates are necessary.

Recently, our group used interfacial sites in combination with nanoconfinement to break scaling laws through the development of cascade nanozymes and demonstrated the formation of C_3 products, such as propanol, from the CO_2RR at −0.6 V (RHE), which is the lowest overpotential for C_3 products reported to date.[4b] The nanozymes consist of nanoparticles with a Ag core and porous Cu shell. CO_2 diffuses to the Ag core, where it is reduced to CO at low overpotentials with high faradaic efficiency. High local concentrations of CO build up within the porous Cu shell and lead to enhanced C–C coupling between the C_2 products and CO. Products can be selectivity tuned by changing the retention time of the intermediates and local concentration of CO.[35] This is analogous to cascade reactions in enzymes achieved by substrate channeling, which is the direct transfer of an intermediate from one active site to another without entering the bulk solution. The nanoconfinement-induced cascade reaction is observed in a "potential window" where the overpotential is sufficient to convert the CO formed on the Ag sites into higher order products at the Cu sites inside the porous shell, but not too high that the CO_2RR is mostly happening directly at the Cu sites in the nanozyme outer surface (Figure 6b). In the "nanozyme window" (−0.60 to −0.65 V), higher order products, such as *n*-propanol (Figure 6c), are produced at very low overpotentials.

6. Conclusion and Outlook

With the development of techniques to fabricate nanoporous materials with fine-control of morphologies, nanoconfinement is becoming progressively more important in

electrochemistry. However, at present, we only have a nascent understanding of the importance of nanoconfinement in electrochemistry and the impact it can have on improving electrocatalysis. A few studies have investigated how the nature of the electrolyte in nanoconfined spaces changes during an electrochemical reaction. Similarly, there have been only a few investigations that have looked at how nanoconfinement influences the kinetics and selectivity of these reactions. From these initial studies there are already some hints that nanoconfinement can have a profound influence on electrochemical reactions. We have learnt that, in nanoconfined spaces, the structure of water can change, which can impact the mass-transport processes in these nanoconfined spaces.[18,26,27,28c] Similarly, the size of the spaces can cause some species to be excluded simply based on their size,[3b] whereas overlapping diffuse electrical double layers in highly confined spaces can result in species being brought into or expelled from the channels by migration.[4a,15,25] This can then result in very different concentrations of species in the nanoconfined spaces compared with the situation when there is no confinement. These different concentrations of species can be advantageous or deleterious for driving electrocatalytic reactions. The different concentrations of species inside nanoconfined spaces have also been suggested to cause the enhanced adsorption of reactive species, to facilitate overcoming scaling laws, and to drive bimolecular reactions.

Questions remain, however, regarding the reasons for the improved reaction kinetics observed in some nanoconfined systems. For example, nanoconfined spaces often have high curvature, which could suggest that the enhanced reaction kinetics can be attributed to strain effects rather than solution effects. To resolve such ambiguity, better defined experimental systems are required that can allow studies to be guided by theoretical investigations. As described above, the nanoconfined systems can be classified according to the degrees of freedom the solution species possess in the nanoconfined system. Isolated channels, where each channel is its own diffusional system, have the least degrees of freedom and we feel that they are the most suited for understanding the impact of nanoconfinement. We have shown that the greater degrees of nanoconfinement in these systems result in higher specific activity.[4a,15] However, achieving an even more unambiguous understanding of how to exploit nanoconfinement to improve electrocatalysis requires experimental systems to be developed with less heterogeneity in the size and depth of the isolated nanoconfined channels than we have achieved in etched nanoparticles. Fortuitously, nanoconfined channels in metals and silica formed from surfactant self-assembly have been developed for capacitors, sensing, and other applications which appear to have much better control over the size and distribution of nanoconfined channels.[17,36] We are currently exploring these systems to further improve our understanding of nanoconfinement. Combining such well-defined nanoconfined structures with modeling at the nanoscale (e.g. molecular dynamic simulations) will make it possible to achieve a deeper understanding of the different aspects affecting electrochemical reactions in nanoconfined spaces.

One of the reasons for gaining a greater understanding of nanoconfinement in electrochemistry is to be able to exploit it for electrocatalysis. Our own studies have shown that isolated nanoconfined channels are not only the best experimental system for understanding the importance of nanoconfinement, but also that the specific activity for some electrocatalytic reactions are greatest in these systems. This, however, does not mean that such systems are the most ideal for exploiting confinement in industrial processes, because the actual electrocatalytic surface area of these isolated channel systems may in fact be significantly smaller than, for example, mesoporous particles, such that the mass activity is lower. As such, our thinking is that the fundamental knowledge obtained from the isolated nanoconfined systems will be exploited as one aspect in the design of higher surface area, high-performing, electrocatalytic materials. We see nanoconfinement as a complement to the more common approaches to electrocatalysis design focused around the electrocatalytic sites and the adsorption energies involved in reactions at these sites.

Acknowledgements

We acknowledge funding from the Australian Research Council Discovery Grants (R.D.T., DP190102659 and DP200100143; J.J.G., DP210102698). W.S. acknowledges funding from the Deutsche Forschungsgemeinschaft (DFG, German Research Foundation) under Germany's Excellence Strategy—EXC 2033–390677874—RESOLV. J.W. and S.V.S. acknowledge support from the Australian Government Research Training Program (RTP) Scholarship. Open access publishing facilitated by University of New South Wales, as part of the Wiley - University of New South Wales agreement via the Council of Australian University Librarians.

Conflict of Interest

The authors declare no conflict of interest.

Keywords: Electrocatalysis · Electrochemistry · Ion Migration · Nanotechnology · Scaling Relationships

[1] J. H. Montoya, L. C. Seitz, P. Chakthranont, A. Vojvodic, T. F. Jaramillo, J. K. Nørskov, *Nat. Mater.* **2017**, *16*, 70–81.

[2] a) K. Chang, X. Jian, H. M. Jeong, Y. Kwon, Q. Lu, M.-J. Cheng, *J. Phys. Chem. Lett.* **2020**, *11*, 1896–1902; b) M. Nesselberger, M. Roefzaad, R. F. Hamou, P. U. Biedermann, F. F. Schweinberger, S. Kunz, K. Schloegl, G. K. H. Wiberg, S. Ashton, U. Heiz, K. J. J. Mayrhofer, M. Arenz, *Nat. Mater.* **2013**, *12*, 919–924; c) Y. Zhou, W. Chen, P. Cui, J. Zeng, Z. Lin, E. Kaxiras, Z. Zhang, *Nano Lett.* **2016**, *16*, 6058–6063; d) Y. Yao, Q. Fu, Y. Zhang, X. Weng, H. Li, M. Chen, L. Jin, A. Dong, R. Mu, P. Jiang, *Proc. Natl. Acad. Sci. USA* **2014**, *111*, 17023–17028; e) Y. Zhang, X. Weng, H. Li, H. Li, M. Wei,

J. Xiao, Z. Liu, M. Chen, Q. Fu, X. Bao, *Nano Lett.* **2015**, *15*, 3616–3623; f) A. D. Doyle, J. H. Montoya, A. Vojvodic, *ChemCatChem* **2015**, *7*, 738–742.
[3] a) M. Ma, K. Djanashvili, W. A. Smith, *Angew. Chem. Int. Ed.* **2016**, *55*, 6680–6684; *Angew. Chem.* **2016**, *128*, 6792–6796; b) J. Ding, X. Li, L. Zhou, R. Yang, F. Yan, B. Su, *J. Mater. Chem. B* **2020**, *8*, 3616–3622.
[4] a) J. Wordsworth, T. M. Benedetti, A. Alinezhad, R. D. Tilley, M. A. Edwards, W. Schuhmann, J. J. Gooding, *Chem. Sci.* **2020**, *11*, 1233–1240; b) P. B. O'Mara, P. Wilde, T. M. Benedetti, C. Andronescu, S. Cheong, J. J. Gooding, R. D. Tilley, W. Schuhmann, *J. Am. Chem. Soc.* **2019**, *141*, 14093–14097; c) E. E. Benn, B. Gaskey, J. D. Erlebacher, *J. Am. Chem. Soc.* **2017**, *139*, 3663–3668; d) T.-T. Zhuang, Y. Pang, Z.-Q. Liang, Z. Wang, Y. Li, C.-S. Tan, J. Li, C. T. Dinh, P. De Luna, P.-L. Hsieh, T. Burdyny, H.-H. Li, M. Liu, Y. Wang, F. Li, A. Proppe, A. Johnston, D.-H. Nam, Z.-Y. Wu, Y.-R. Zheng, A. H. Ip, H. Tan, L.-J. Chen, S.-H. Yu, S. O. Kelley, D. Sinton, E. H. Sargent, *Nat. Catal.* **2018**, *1*, 946–951.
[5] a) W. Schmickler, E. Santos, *Interfacial electrochemistry*, Springer Science & Business Media, Cham, **2010**, pp. 165–167; b) J. K. Nørskov, F. Studt, F. Abild-Pedersen, T. Bligaard, *Fundamental concepts in heterogeneous catalysis*, Wiley, Hoboken, **2014**, pp. 85–105.
[6] H. Ooka, J. Huang, K. S. Exner, *Front. Energy Res.* **2021**, https://doi.org/10.3389/fenrg.2021.654460.
[7] J. H. Bae, J.-H. Han, T. D. Chung, *Phys. Chem. Chem. Phys.* **2012**, *14*, 448–463.
[8] Z. Li, C. Yu, Y. Wen, Y. Gao, X. Xing, Z. Wei, H. Sun, Y.-W. Zhang, W. Song, *ACS Catal.* **2019**, *9*, 5084–5095.
[9] a) S. Fleischmann, M. A. Spencer, V. Augustyn, *Chem. Mater.* **2020**, *32*, 3325–3334; b) M. Seo, T. D. Chung, *Curr. Opin. Electrochem.* **2019**, *13*, 47–54.
[10] a) Y. I. Hori, *Modern aspects of electrochemistry*, Springer, Heidelberg, **2008**, pp. 89–189; b) S. Nitopi, E. Bertheussen, S. B. Scott, X. Liu, A. K. Engstfeld, S. Horch, B. Seger, I. E. Stephens, K. Chan, C. Hahn, *Chem. Rev.* **2019**, *119*, 7610–7672.
[11] M. Myekhlai, T. M. Benedetti, L. Gloag, A. R. Poerwoprajitno, S. Cheong, W. Schuhmann, J. J. Gooding, R. D. Tilley, *Chem. Eur. J.* **2020**, *26*, 15501–15504.
[12] a) G. Sun, J. Wang, X. Liu, D. Long, W. Qiao, L. Ling, *J. Phys. Chem. C* **2010**, *114*, 18745–18751; b) S. Park, Y. J. Song, J.-H. Han, H. Boo, T. D. Chung, *Electrochim. Acta* **2010**, *55*, 2029–2035.
[13] J. Snyder, T. Fujita, M. Chen, J. Erlebacher, *Nat. Mater.* **2010**, *9*, 904–907.
[14] K. D. Yang, W. R. Ko, J. H. Lee, S. J. Kim, H. Lee, M. H. Lee, K. T. Nam, *Angew. Chem. Int. Ed.* **2017**, *56*, 796–800; *Angew. Chem.* **2017**, *129*, 814–818.
[15] T. M. Benedetti, C. Andronescu, S. Cheong, P. Wilde, J. Wordsworth, M. Kientz, R. D. Tilley, W. Schuhmann, J. J. Gooding, *J. Am. Chem. Soc.* **2018**, *140*, 13449–13455.
[16] G. Zhou, B. Wang, R. Cao, *J. Am. Chem. Soc.* **2020**, *142*, 14848–14853.
[17] a) G. S. Attard, P. N. Bartlett, N. R. Coleman, J. M. Elliott, J. R. Owen, J. H. Wang, *Science* **1997**, *278*, 838–840; b) P. N. Bartlett, *Electrochem. Soc. Interface* **2004**, *13*, 28–33.
[18] a) R. H. Tunuguntla, R. Y. Henley, Y.-C. Yao, T. A. Pham, M. Wanunu, A. Noy, *Science* **2017**, *357*, 792–796; b) R. H. Tunuguntla, F. I. Allen, K. Kim, A. Belliveau, A. Noy, *Nat. Nanotechnol.* **2016**, *11*, 639–644.
[19] a) S.-M. Lu, Y.-Y. Peng, Y.-L. Ying, Y.-T. Long, *Anal. Chem.* **2020**, *92*, 5621–5644; b) Y.-L. Ying, Y.-T. Long, *J. Am. Chem. Soc.* **2019**, *141*, 15720–15729.
[20] a) J.-H. Han, E. Lee, S. Park, R. Chang, T. D. Chung, *J. Phys. Chem. C* **2010**, *114*, 9546–9553; b) J. H. Bae, J.-H. Han, D. Han, T. D. Chung, *Faraday Discuss.* **2013**, *164*, 361–376.
[21] C.-H. Hou, P. Taboada-Serrano, S. Yiacoumi, C. Tsouris, *J. Chem. Phys.* **2008**, *128*, 044705.
[22] S. Xue, B. Garlyyev, A. Auer, J. Kunze-Liebhäuser, A. S. Bandarenka, *J. Phys. Chem. C* **2020**, *124*, 12442–12447.
[23] F. Calle-Vallejo, J. Tymoczko, V. Colic, Q. H. Vu, M. D. Pohl, K. Morgenstern, D. Loffreda, P. Sautet, W. Schuhmann, A. S. Bandarenka, *Science* **2015**, *350*, 185–189.
[24] a) K. Fu, S.-R. Kwon, D. Han, P. W. Bohn, *Acc. Chem. Res.* **2020**, *53*, 719–728; b) C. Ma, N. M. Contento, P. W. Bohn, *J. Am. Chem. Soc.* **2014**, *136*, 7225–7228.
[25] Q. Chen, K. McKelvey, M. A. Edwards, H. S. White, *J. Phys. Chem. C* **2016**, *120*, 17251–17260.
[26] G. Hummer, J. C. Rasaiah, J. P. Noworyta, *Nature* **2001**, *414*, 188–190.
[27] O. O. Sofronov, H. J. Bakker, *ACS Cent. Sci.* **2020**, *6*, 1150–1158.
[28] a) S. Sahu, M. Di Ventra, M. Zwolak, *Nano Lett.* **2017**, *17*, 4719–4724; b) L. A. Richards, A. I. Schäfer, B. S. Richards, B. Corry, *Phys. Chem. Chem. Phys.* **2012**, *14*, 11633–11638; c) L. A. Richards, A. I. Schäfer, B. S. Richards, B. Corry, *Small* **2012**, *8*, 1701–1709.
[29] C. Duan, A. Majumdar, *Nat. Nanotechnol.* **2010**, *5*, 848–852.
[30] J. Ma, K. Li, Z. Li, Y. Qiu, W. Si, Y. Ge, J. Sha, L. Liu, X. Xie, H. Yi, *J. Am. Chem. Soc.* **2019**, *141*, 4264–4272.
[31] M. Luo, S. Guo, *Nat. Rev. Mater.* **2017**, *2*, 17059.
[32] J. Masa, W. Schuhmann, *J. Solid State Electrochem.* **2020**, *24*, 2181–2182.
[33] T. Sours, A. Patel, J. Nørskov, S. Siahrostami, A. Kulkarni, *J. Phys. Chem. Lett.* **2020**, *11*, 10029–10036.
[34] J. Huang, M. Mensi, E. Oveisi, V. Mantella, R. Buonsanti, *J. Am. Chem. Soc.* **2019**, *141*, 2490–2499.
[35] P. Wilde, P. OMara, J. R. Junqueira, T. Tarnev, T. Benedetti, C. Andronescu, Y.-T. Chen, R. Tilley, W. Schuhmann, J. J. Gooding, *Chem. Sci.* **2021**, *12*, 4028–4033.
[36] a) A. Walcarius, *Chem. Soc. Rev.* **2013**, *42*, 4098–4140; b) A. Walcarius, E. Sibottier, M. Etienne, J. Ghanbaja, *Nat. Mater.* **2007**, *6*, 602–608.

Manuscript received: January 17, 2022
Accepted manuscript online: April 10, 2022
Version of record online: May 31, 2022